Structural and Optical Properties of Er(III) Complex with ODA and Phen (ODA = Oxydiacetate, Phen = 1,10-Phenanthroline)

Jun-Gill Kang, [*] **Tack-Jin Kim, Kwan Soo Park,** [†] **and Sung Kwon Kang**

Department of Chemistry, Chungnam National University, Daejeon 305-764, Korea
[†]*Korea Water Resources Corporation, Daejeon 305-730, Korea*
Received December 10, 2003

A novel Er(III) complex with oxydiacetate and 1,10-phenanthroline was synthesized and its structure and luminescence properties were characterized. The complex of $[Er(ODA) \cdot (phen) \cdot 4H_2O]^+$ crystallizes in the monoclinic space group $P2_1/n$ with $a = 12.216(4)$ Å, $b = 16.680(2)$ Å, $c = 12.627(3)$ Å, $\beta = 108.30(2)°$, V = 2442.7(11) Å^3, Z = 4 and $\rho = 1.841$ g/cm^3. When the complex is excited at the He-Cd 325-nm line, it produces two broad bands spanning the regions 350-650 nm and 1200-1650 nm. The emission band of the complex is characterized by a series of spectral dips in the visible emission profile. The complex exhibits sensitized near-IR emission via two kinds of energy transfers from phen to Er(III): nonradiative and radiative energy transfers.

Key Words : $[Er(ODA) \cdot (phen) \cdot 4H_2O]^+$, X-ray structure, Photoluminescence, Spectral dip, Energy transfer

Introduction

Trivalent erbium ions in different host environment have attracted great interest for their potential usefulness in display and semiconductor technologies and fiberoptic communication.[1-6] Such applications are based primarily on the 1.54-μm emission from Er-doped inorganic materials. Recently, two Er(III) complexes, tris(8-hydroxyquinoline) erbium(III)[7] and tris(acetylacetonato)(1,10-phenanthroline)-erbium(III),[8] were synthesized and their photoluminescence (PL) and electroluminescence (EL) were tested. We are interested in synthesizing and characterizing lanthanide complexes with mixed polycarboxylate and 1,10-phenan-throline(phen) ligands. We prepared Er(III) complex using oxydiacetate (ODA) as a chelate and phen as a sensitizer, and characterized its structure and luminescence properties. To the best of our knowledge, lanthanide complexes with mixed polycarboxylate and phen ligands have not been reported yet. Only x-ray structures of nickel and zinc with mixed ODA and phen,[9] and the crystal free-ion energy level of Er complex with ODA have been reported.[10]

Experimental Section

Crystal Growth and Composition Analysis. ErNO$_3$·6H$_2$O (99.9%), oxydiacetic acid (ODAH$_2$, 98%) and 1,10-phenamthroline (phen, 99+ %) were purchased from Aldrich and used without further purification. ODAH$_2$ (0.268 g, 2 mmol) was added to a solution of erbium nitrate hexahydrate (0.381 g, 1 mmol) and phen (0.180 g, 1 mmol) in water (10 mL). The pH of the solution was adjusted to between 5 and 6 with dilute NaOH and the resultant solution was stirred for 2 h at room temperature. The resultant solution was initially pink, but changed to orange. Pink prismatic crystals of the complex were obtained by the slow evaporation method.

The cations were analyzed quantitatively with a Perkin-Elmer 2380 atomic absorption spectrometer. The carbon, hydrogen, nitrogen and oxygen contents were analyzed on a CE EA-1110 elemental analyzer. Ion chromatographic analysis was used to determine the amount of chloride ion in the crystals. Anal. Found: Er 25.2; C 28.4; H 4.4; N 4.2; Cl 5.3%. Cal. For Er(ODA)(phen)Cl·9H$_2$O: Er 24.7; C 28.4; H 4.5; N 4.2; Cl 5.3%.

Determination and Refinement of the X-ray Structure. X-ray crystallography on the single crystal specimen of [Er(ODA)(phen)·4H$_2$O]Cl·5H$_2$O was performed on a Bruker P4 diffractometer with graphite monochromated Mo Kα radiation. Intensity data were collected at room temperature using the ω-θ scan technique. The data were corrected for Lorentz-polarization effects, and empirical absorption correction (Ψ scan) was also applied. The structures of the titled compounds were solved by applying the direct method using Bruker SHELXTL[11] and refined by a full-matrix least-squares refinement on F using SHELEX97.[12] The non-H atoms were refined with anisotropic displacement parameters. Hydrogen atoms were fixed at ideal geometric positions, and their contributions were included in the structural factor calculations. The crystal data and refinement results are summarized in Table 1.

Optical Measurements. For measurements of lumine-scence and excitation spectra in visible region single crystals were placed on the cold finger of a CTI-cryogenics using silicon grease. The spectra were measured at 90° angle with an ARC 0.5 m Czerny-Turner monochromator equipped with a cooled Hamamatsu R-933-14 PM tube. The sample was irradiated with an He-Cd 325-nm laser line or the light from an Oriel 1000 W Xe lamp (working power, 400 W) passing through an Oriel MS257 monochromator. Photo-luminescence (PL) spectrum in the near-IR (NIR) region was measured with a SPEX double monochromator equipp-ed with a L-N$_2$ cooled Ge detector.

Table 1. Crystal data and structure refinement for [Er(ODA)-(phen)·4H₂O]Cl·5H₂O

Empirical formula	C16 H30 Cl Er N2 O14
Formula weight	677.13
Temperature	293(2) K
Wavelength	0.71073 Å
Crystal system	Monoclinic
Space group	$P2_1/n$
Unit cell dimensions	a = 12.216(4) Å α = 90.0°
	b = 16.680(2) Å β = 108.30(2)°
	c = 12.627(3) Å γ = 90.0°
Volume	2442.7(11) Å³
Z	4
Density(calculated)	1.841 g/cm³
Absorption coefficient	3.615 mm⁻¹
F(000)	1348
Crystal size	0.46 × 0.42 × 0.36 mm³
Theta range for data collection	2.02 to 27.47°
Index ranges	-15 ≤ h ≤ 15, 0 ≤ k ≤ 21, 0 ≤ l ≤ 16
Reflections collected	5836
Independent reflections	5592 [R(int) = 0.0156]
Completeness to theta = 27.47°	99.9%
Absorption correction	Psi-scan
Max. and min. transmission	0.8239 and 0.5259
Refinement method	Full-matrix least-squares on F²
Data / restraints / parameters	5592 / 0 / 320
Goodness-of-fit on F²	1.047
Final R indices [I>2sigma(I)]	R1 = 0.0297, wR2 = 0.0688
R indices (all data)	R1 = 0.0388, wR2 = 0.0723
Extinction coefficient	0.00147(14)
Largest diff. peak and hole	1.730 and -0.699 e.Å⁻³

Results and Discussion

Description of Structure. The titled compound crystallizes in the monoclinic space $P2_1/n$. Figure 1 shows the perspective view of the crystalline form of [Er(ODA)(Phen)·4H₂O]⁺ complex. Selected bond lengths and angles are given in Table 2. As shown in Figure 1, the Er(III) ion satisfies nine-coordination via binding to a tridentate ODA, bidentate phen and four water molecules. The Er-O distances are 2.289(3) and 2.312(3) Å for two Er-carboxylate oxygen bonds, and 2.493(3) Å for the Er-ether oxygen bond. These values are in good agreement with the average values of Ln-O distances of [Ln(ODA)₃]³⁻ (Ln = Nd, Gd, and Yb): 2.31-2.37 Å for Ln-carboxylate oxygen bonds and 2.46-2.52 Å for Ln-ether oxygen bonds.[13] The Er-N distances are 2.543(3) and 2.549(3) Å. These values are also in good agreement with the values of 2.538(6) and 2.526(5) Å of [Er(hfpd)₂(μ-OCH₃)(phen)]₂.[14] The angle formed by Er and two carboxylate oxygen atoms is 126.60(11)°, which is in good agreement with the values of 126-129° of [Ln(ODA)₃]³⁻ (Ln = Nd, Gd, and Yb). A characteristic feature of the geometry of the titled complex is seen in the two carboxylate oxygen atoms of ODA and the two nitrogen atoms of phen. The least-square equation for the plane formed by these four
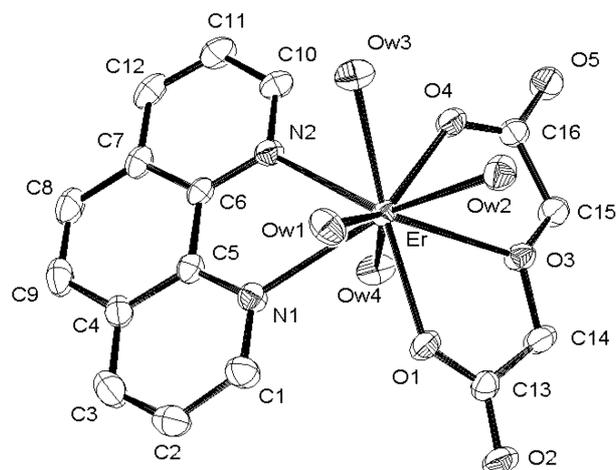
Figure 1. View of the [Er(ODA)(Phen)·4H₂O]⁺ cation with atom labeling and ellipsoids at 50%. Hydrogen atoms have been omitted for clarity.

atoms is $0.2342x + 16.5139y + 1.599z = 2.8486$. The displacements of these atoms from their mean plane are less than 0.003 Å, which shows that these four form a perfect rectangular plane within the limits of uncertainty. Nine-coordinated Ln(III) complexes most frequently form a tri-capped trigonal prism (TCTP) polyhedron, while the capped square antiprism (CSAP) polyhedron is rare. In Figure 1, the TCTP geometry results from the three rectangular (O1-Ow4-O4-Ow2, O1-Ow4-N2-Ow1, Ow2-O4-N2-Ow1) and the two triangular (O1-Ow1-Ow2, Ow4-N2-O4) faces of the trigonal prism and the three atoms occupying the capping

Table 2. Bond lengths (Å) and angles (°) for [Er(ODA)(phen)·4H₂O]Cl·5H₂O

Er-O(1)	2.289(3)	Er-O(4)	2.312(3)
Er-OW1	2.379(3)	Er-OW3	2.413(3)
Er-OW4	2.416(3)	Er-OW2	2.445(3)
Er-O(3)	2.493(3)	Er-N(2)	2.543(3)
Er-N(1)	2.549(3)		
O(1)-Er-O(4)	128.06(10)	O(1)-Er-OW1	78.08(10)
O(4)-Er-OW1	139.53(10)	O(1)-Er-OW3	143.93(10)
O(4)-Er-OW3	72.36(10)	OW1-Er-OW3	70.74(10)
O(1)-Er-OW4	82.46(10)	O(4)-Er-OW4	77.13(11)
OW1-Er-OW4	142.34(11)	OW3-Er-OW4	133.58(10)
O(1)-Er-OW2	82.70(11)	O(4)-Er-OW2	80.34(11)
OW1-Er-OW2	72.60(10)	OW3-Er-OW2	71.18(10)
OW4-Er-OW2	136.27(11)	O(1)-Er-O(3)	63.39(9)
O(4)-Er-O(3)	64.73(9)	OW1-Er-O(3)	126.82(10)
OW3-Er-O(3)	123.91(10)	OW4-Er-O(3)	68.94(10)
OW2-Er-O(3)	67.62(10)	O(1)-Er-N(2)	135.74(11)
O(4)-Er-N(2)	79.29(11)	OW1-Er-N(2)	103.33(11)
OW3-Er-N(2)	70.76(11)	OW4-Er-N(2)	69.82(11)
OW2-Er-N(2)	140.71(10)	O(3)-Er-N(2)	129.81(10)
O(1)-Er-N(1)	75.15(11)	O(4)-Er-N(1)	139.11(11)
OW1-Er-N(1)	70.66(10)	OW3-Er-N(1)	109.76(11)
OW4-Er-N(1)	73.33(11)	OW2-Er-N(1)	140.14(10)
O(3)-Er-N(1)	126.29(10)	N(2)-Er-N(1)	64.38(11)

positions (O3, N1, Ow3). The dihedral angles (δ) between pairs of adjacent triangular faces, O3(O1Ow4)N1, N1(Ow1N2)Ow3 and Ow3(O4Ow2)O3, were calculated at 31.09(16), 5.62(24) and 33.81(12)°, respectively. Significant deviation from the ideal TCTP geometry in the range of 25°-30° occurs in the 5.17(28)° of N1(Ow1N2)Ow3. This dihedral angle implies that N1, Ow2, N2 and Ow3 may be almost planar. The least-square equation for this plane is $0.2342x + 16.5139y + 1.599z = 2.8486$. The displacements of these atoms from their mean plane are 0.049-0.050 Å, indicating that the geometry of [Er(ODA)(Phen)·4H$_2$O]$^+$ complex is a slightly distorted CASP.

Photoluminescence. The PL spectrum of [Er(ODA)-(Phen)·4H$_2$O]$^+$ excited at the 325 nm He-Cd line was measured at wavelengths from 350 to 1650 nm at various temperatures. As shown in Figure 2, the complex produces two broad bands spanning 350-650 nm and 1200-1650 nm regions. The visible luminescence band is strikingly different from the green emission bands of Er(III), reported previously.[7] The characteristic feature of its emission band is a series of spectral dips in the emission profile seen at 377, 408, 442, 450, 490, 522, 541 and 654 nm (labeled dips 1, 2, 3, 4, 5, 6, 7 and 8, respectively). Some accompany satellite dips. As shown in Figure 2(a), the intensity of the visible emission band of [Er(ODA)(Phen)·4H$_2$O]$^+$ decreases remarkedly with increasing temperature. However, the
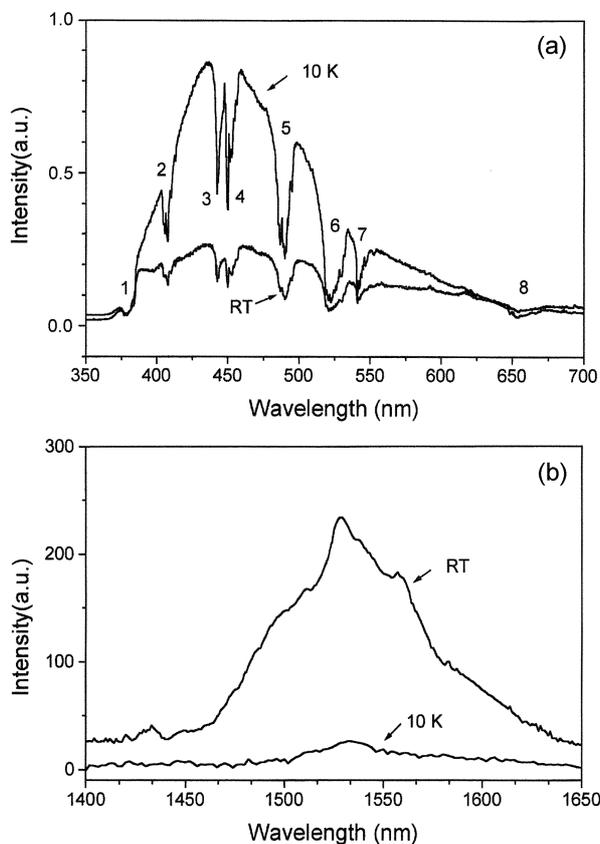
spectral dips persist up to room temperature. The relative depth of each dip is nearly independent on the temperature. By contrast, the temperature dependence of the NIR emission band is quite different from that of the visible emission band. At 10 K, unlikely, 325-nm excitation produces only a trace in the NIR region, while at room temperature this NIR emission band is much more intense, forming a well-shaped band structure that peaks at 1530 nm, as shown in Figure 2(b).

To examine whether these dips are associated with the Er(III) ion in the complex, the reflectance spectrum of the complex was measured at room temperature in the wavelength range from UV to NIR. As shown in Figure 3, characteristic bands appeared in the 360-1650 nm region, these are attributed to the f → f transitions of Er(III) in the complex. As illustrated in Figures 2(a) and 3, the peaks of the reflectance bands coincide exactly with the locations of the spectral dips. Surprisingly, the dips in the visible luminescence result from the electronic transitions of trivalent erbium ions. Of the observed dips in the PL spectrum, the 522-nm dip has the largest relative depth. This band and the 1512 nm band appeared as the largest in the reflectance spectrum. Taking into account the energy-level scheme for Er(III),[15] this experimental evidence indicates that dip 6 locating at 522 nm, which is attributed to the transition from the ground $^4I_{15/2}$ state to the exited $^2H_{11/2}$ state, is hypersensitive. In addition to the 522-nm band, the 379-nm band, attributed to the transition from the ground $^4I_{15/2}$ state to the exited $^4G_{11/2}$ state, might show hypersensitivity, since a value of $U^{(2)}$ matrix element for this transition is as large as that for the $^4I_{15/2} \rightarrow {}^2H_{11/2}$ transition.[15] The 442-nm band did not appear in the reflectance spectrum, but it presented as a dip with the relative depth of 0.49. Considering the energy-level scheme of the free Er(III) ion, this dip likely results from the $^4I_{15/2} \rightarrow {}^4F_{3/2}$ transition. Accordingly, the observed extraordinary spectral dips in the PL spectrum arise from the radiative energy transfer from phen or ODA to the Er(III) ion in the complex.

Figure 2. PL spectra of [Er(ODA)(Phen)·4H$_2$O]$^+$ scanned in: (a) the visible and (b) near IR regions and measured at 10 K and room temperature.
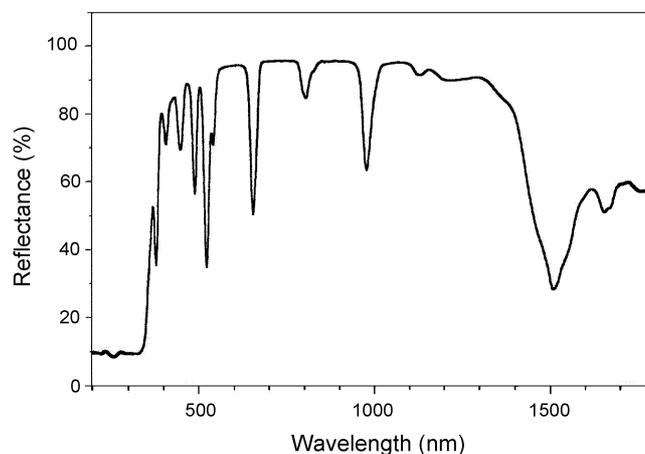
Figure 3. Reflectance spectrum of [Er(ODA)(Phen)·4H$_2$O]$^+$ measured at room temperature. Anhydrous barium sulfate is used as the standard.
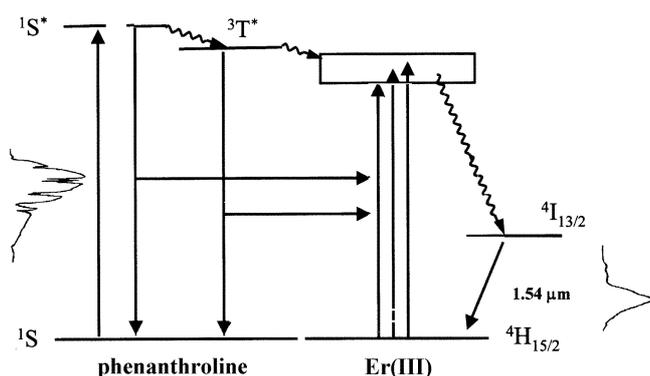
Figure 4. A schematic diagram of the near-IR emission from [Er(ODA)(Phen)·4H$_2$O]$^+$ resulting from radiative and nonradiative energy transfers from 1,10-phenanthroline to Er(III).

PL spectra of phen and Na$_3$ODA in crystalline states were also measured at 10 K and room temperature to examine whether the observed visible luminescence originated from phen or ODA. Both produced broad bands spanning the 350-700-nm wavelength region. However, the phen band is more than 20 times more intense than that of Na$_3$ODA. It indicates that phen is responsible for the band observed in the visible region with [Er(ODA)(Phen)·4H$_2$O]$^+$, although phen is a good sensitizer for the nonradiative energy transfer to a coordinated rare earth ion.

Radiative and Nonradiative Energy Transfers. When the complexes are excited at 325 nm, the observed near-IR emission, attributed to the $^4I_{13/2} \rightarrow {}^2H_{11/2}$ transition, is produced predominantly *via* energy transfer from the ligands to the Er(III) ion in the complex, since there is no strong absorption band around 325 nm for Er(III). The energy transfer from the ligand to the metal (ETLM) is primarily nonradiative. However, for [Er(ODA)(phen)·4H$_2$O]$^+$ the ETLM is both nonradiative and radiative via the ligands. When [Er(ODA)(Phen)·4H$_2$O]$^+$ is excited at 325 nm, phen absorbs photons. Mostly, the nonradiative ETLM process takes place from the excited states of phen to the excited states of Er(III) at lower levels and results in the NIR luminescence. In addition, competing with the nonradiative ETLM, radiative transitions in phen take place from the excited states to the ground state as fluorescence and phosphorescence. The Er(III) ion coordinated with phen and ODA ligands absorbs some photons emitted from the ligand

phen. This reabsorption results in the series of spectral dips in the fluorescence and phosphorescence spectra of phen. For phen, the nonradiatve ETLM is much more favorable than the radiative transitions even at low temperature. Consequently, NIR emission from Er(III) is favorably induced in [Er(ODA)(Phen)·4H$_2$O]$^+$. These processes are illustrated occurring in [Er(ODA)(Phen)·4H$_2$O]$^+$ in Figure 4.

References

1. Mita, Y. In *Phosphor Handbook*; Shionoya, S.; Yen, W. M., Eds.; CRC Press: New York, 1999; Chap 12.
2. Ennen, H.; Pomrenke, G.; Axmann, A.; Eisele, K.; Haydl, W.; Schneider, W. *Appl. Phys. Lett.* **1985**, *46*, 381.
3. Coffa, S.; Franzò, G.; Priolo, F.; Polman, A.; Serna, R. *Phys. Rev. B* **1994**, *49*, 16313.
4. Stepikhova, M.; Palmetshofer, L.; Jantsch, W.; von Bardeleben, H. J.; Gaponenko, N. V. *Appl. Phys. Lett.* **1999**, *74*, 537.
5. Kozanecki, A.; Sealy, B. J.; Homewood, K. *J. Alloy Comp.* **2000**, *300-301*, 61.
6. Xiao, Z.; Xu, F.; Zhang, T.; Cheng, G.; Gu, L.; Wan, X. *J. Lumin.* **2002**, *96*, 195.
7. Curry, R. J.; Gillin, W. P. *Appl. Phys. Lett.* **1999**, *75*, 1380.
8. Sun, R. G.; Wang, Y. Z.; Zheng, Q. B.; Zhang, H. J.; Epstein, A. J. *J. Appl. Phys.* **2000**, *87*, 7589.
9. Baggio, R.; Garland, M. T.; Perec, M. *J. Chem. Soc. Dalton Trans.* **1996**, 2747.
10. *SHELXTL*, 5.030 ed.; Brucker Analytical X-ray Instruments, Inc.; Madison, WI, 1998.
11. Rukmini, E.; Devi, R.; Jayasankar, C. K. *Phys. B* **1994**, *193*, 166.
12. Sheldrick, G. M. *SHELEX97*; University of Göttingen: 1997.
13. Albertsson, J. *Acta Chem. Scand.* **1968**, *22*, 1562.
14. van Staveren, D. R.; Haasnoot, J. G.; Lanfredi, A. M. M.; Menzer, S.; Niewenhuizen, P. J.; Spek, A. L.; Ugozzoli, F.; Reedijk, J. *Inorg. Chim. Acta* **2000**, *307*, 81.
15. Reisfeld, R.; Jørgensen, C. K. In *Lasers and Excited States of Rare Earths*; Springer-Verlag: Berline, 1977; Chap. 3.